High-repetition rate and coherent free-electron laser in the tender x rays based on the echo-enabled harmonic generation of an ultraviolet oscillator pulse

N. S. Mirian,[1,*] M. Opromolla,[2,3,†] G. Rossi,[2] L. Serafini,[3] and V. Petrillo[2,3]

[1]*Deutsches Elektronen-Synchrotron DESY, 22607 Hamburg, Germany*
[2]*Università degli Studi di Milano, Via Celoria, 16 20133 Milano, Italy*
[3]*INFN - Sezione di Milano, Via Celoria 16, 20133 Milano and LASA, Via F. Cervi 201, 20090 Segrate (MI), Italy*

(Received 1 October 2020; accepted 3 May 2021; published 27 May 2021)

Fine time-resolved analysis of matter—i.e., spectroscopy and photon scattering—in the linear response regime requires a fs-scale pulsed, high repetition rate, fully coherent x-ray source. A seeded free-electron laser (FEL) driven by a super-conducting linac, generating 10^8–10^{10} coherent photons at 2–5 keV with about 0.5 MHz of repetition rate, can address this need. The seeding scheme proposed is the echo-enabled harmonic generation, alimented by a FEL oscillator working at 13.6 nm with a cavity based on Mo-Si mirrors. The whole chain of the x-ray generation is here described by means of start-to-end simulations. Comparisons with the self-amplified spontaneous emission and a fresh-bunch harmonic cascade performed with similar electron beams show the validity of this scheme.

DOI: 10.1103/PhysRevAccelBeams.24.050702

I. INTRODUCTION

Fine time-resolved analysis of matter is currently performed with synchrotron radiation (SR) sources or with x ray free electron lasers (FELs), whose extremely brilliant pulses are able to detect matter in highly excited states dominated by non-linear response. Spectroscopic studies and photoemission experiments require probes with fluxes smaller than 10^8 photons/pulse and MHz-class repetition rates, for remaining below the linear response threshold and collecting adequate statistics. Current FELs' photon number exceeds this level by 2–4 orders of magnitude, requiring severe attenuation with huge waste of energy. On one hand, sources based on warm linacs, operating at 10/120 Hz, are inadequate for collecting statistics for high resolution spectroscopy. On the other hand, signals like the one by EuXFEL [1,2], shaped in thousands micropulses grouped in 10 macropulses per second, are also nonideal for spectroscopy as both attenuation is needed and the high repetition rate of the micropulses overruns detector and pump-probe set-up capability. SASE fluctuations severely limit the use of FELs in x-ray spectroscopy and full seeding, routinely implemented at FERMI@Elettra [3] and SXFEL [4], should be extended to tender/hard x-ray energies.

There is therefore scientific need and ample room for a novel type of source: a source delivering to the sample 10^7–10^8 photons in 10 fs coherent pulses at 0.5–2 MHz in the tender/hard x-ray range, thus bridging the gap in time resolution and average photon flux between the most advanced SR and the current FELs. These requests are addressed by conceiving a tailored seeded FEL driven by Linacs based on Super-Conducting cavities, providing 10^8–10^{10} coherent photons at 2–5 keV, at about 1 MHz of repetition rate. In the seeded FEL configuration, an external coherent pulse imprints its temporal phase on the electron beam at the undulator entrance. The direct seeding [5] is not possible in the soft-hard x-ray range due to the lack of high-power coherent seeds at these wavelengths, while self-seeding processes [6,7] only achieve partial coherence. High gain harmonic generation (HGHG) multistage cascades [8], seeded by the harmonics of an IR laser generated in crystals [9] or in gases [10–13], have been demonstrated and applied up to few nm wavelengths [3]. However, their implementation in the tender/hard x-ray range is highly demanding, while the extension to higher repetition rates, obtained by using oscillators [14] or lasers in cavity [15], has been studied sofar only theoretically. As demonstrated at SXFEL [4], a step toward high repetition rate seeded FELs is also foreseen by using an optical klystronlike configuration, allowing us to reduce the requirement for the peak power of the seed laser. FEL oscillators [16–21] or regenerative amplifiers [22–26]

*najmeh.mirian@desy.de
†Michele.Opromolla@mi.infn.it

could directly produce coherent x rays [14,27], but the operational scenario proposed so far, with electrons at several GeVs, impedes their realization in small/medium size research laboratories. UV/soft x-ray coherent radiation has been generated with the echo-enabled harmonic generation (EEHG) [28–32], a technique which requires two coherent radiation pulses, usually delivered by optical lasers, seeding the electron beam in two sequential modulators interspersed by a strong dispersive section. A second dispersive section and the radiator are placed downstream. As explained in Refs. [28,29], the combination of energy modulation and dispersion, replicated twice, warps the electron longitudinal phase space, producing a significant bunching on very high harmonics which drives the emission of a short wavelength coherent pulse in the radiator. A combined EEHG-oscillator scheme with two oscillators as modulators has also been proposed [33].

In this paper, we show the operation of a FEL in the tender X-ray range, based on EEHG. We propose a FEL Oscillator in the far ultraviolet frequency range as seeding source. The advantage of such a scheme is twofold: the oscillator operation, combined with an electron beam accelerated in a superconducting linac, increases the device repetition rate by many orders of magnitude (4–6). Moreover, since the oscillator frequency and peak power are much higher than the ones of a conventional laser, the soft-hard x-ray range can be more easily reached by a lower harmonic number.

II. LAYOUT OF THE COHERENT SOURCE AND SIMULATIONS

The electron beam is supposed to be generated by an accelerator similar to the project MariX's (multidisciplinary advanced research infrastructure for the generation and application of x rays) [34,35], whose compact footprint with a total length of about 500 m and contained costs should permit its construction also in medium-size research infrastructures or within university campuses. MariX is based on the innovative design of a two-pass two-way superconducting linear electron accelerator [35], equipped with an arc compressor [36,37] to be operated in CW mode at 1 MHz. The characteristics of the electron beam are listed in Table I. As studied and demonstrated in Ref. [38], the superconducting technology allows to achieve low jitters and fluctuations of the electron beam. These increased stability conditions, together with the seeded mode FEL operation, give the possibility to produce a fully coherent, high repetition rate and highly stable x-ray source.

TABLE I. Electron beam for MariX FEL.

Electron beam energy	GeV	2–3.8
Charge	pC	30–50
Current	kA	1.6
rms normalized emittance	mm mrad	0.3–0.5
rms relative energy spread	10^{-4}	3
Electron beam duration	fs	12
Slice energy spread	10^{-4}	4-2
Slice normalized emittance	mm mrad	0.3

Figure 1 shows the scheme of the source. After the acceleration stage, successive electron bunches are alternatively driven in the oscillator or matched to the EEHG undulator device. The electron beam alimenting the oscillator is extracted upstream the linac end at an energy of 2 GeV, while the ones entering the EEHG device may have the same energy or be further accelerated. The oscillator is constituted by a 9 m long undulator segment with period $\lambda_w = 5$ cm and produces 70 μJ of intracavity radiation at $\lambda_O = 13.6$ nm. It is embedded into a folded ring cavity composed by 4 mirrors, two of which focusing, with optics heat loading requiring an intelligent cooling system. For an oscillator repetition rate of 0.5 MHz, the round trip length L_c is 600 m and the distance between two mirrors is $L_c/4 = 150m$. The oscillator supermodes [16] are calculated fully numerically [14,23] by extracting the radiation field simulated by GENESIS1.3 [39] from the oscillator, driving it through the optical line accounting for mirrors and propagation, and superimposing it on the successive electron bunch. The microscopic distribution of the electron beam is changed shot to shot in order to simulate the passage of a sequence of different bunches. After the passage into the oscillator, the electron bunch is deteriorated by the radiation process and driven to the dump.

Figure 2 presents the intracavity pulse temporal and spectral densities of the seed at saturation, whose Table II summarizes the characteristics of the intracavity seed pulse at saturation. After an optical transport line that splits it in two pulses, the seed is synchronized to the electron bunches at the beginning of both modulators. Energy losses along the transport line have been taken into account. The oscillator seed pointing stability and transverse overlap with the electron bunches after the transport line will be checked and adjusted with multipurpose stations and beam stabilization systems as the ones described in [40,41].

To obtain radiation in the range $\lambda = 5 - 2$ Å, namely 2–5 keV, with the MariX's moderate energy electron bunch (2.5–3.8 GeV), a short period radiator must be considered. From the resonance relation $\lambda = \frac{\lambda_w}{2\gamma^2}(1 + a_w^2)$ (a_w is the undulator parameter and γ the electron Lorentz factor), taking a maximum magnetic field $B = 1$ T corresponding to $a_w = 0.98$, we can deduce that an undulator period of $\lambda_w = 1.5$ cm is suitable. Besides, starting from a seed at $\lambda_o = 13.6$ nm, a significant electron bunching on harmonics' order n in the range from 25 to 70 is required. By following the unidimensional model based on plane waves exposed in Ref.s [28,29], the electron bunching is expressed in terms of four free parameters, namely the dispersion strengths of the two chicanes $R_{56,1}$ and $R_{56,2}$ and the normalized electric fields of the seeds:

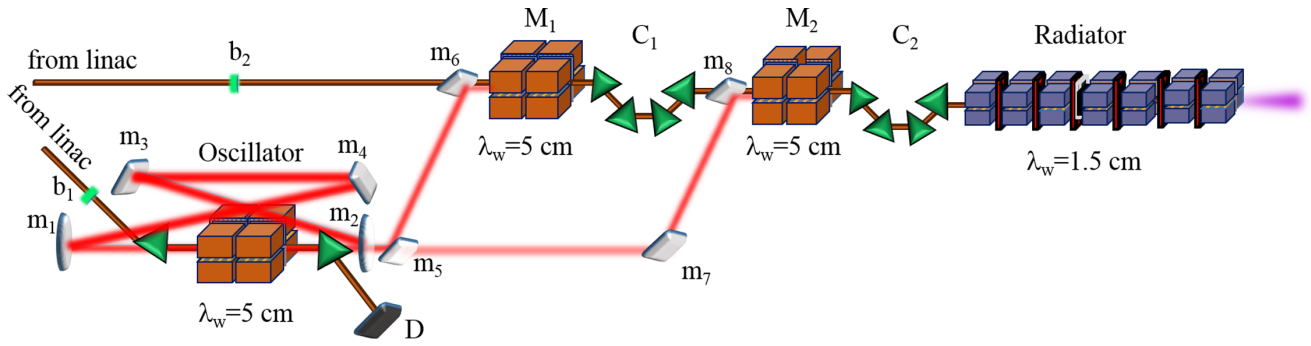

FIG. 1. Scheme of the echo-enhanced harmonic generation FEL. b_1 and b_2: electron bunches alternatively sent in the oscillator and in the undulators. FEL Oscillator undulator: $\lambda_w = 5$ cm, $a_w = 3.71$, total length 9 m. m_1, m_2, m_3, m_4: oscillator cavity mirrors. D: beam dump. m_5, m_6, m_7, m_8: mirrors of the optical line that splits and couples the seed to the modulators. m_2 and m_5: beam splitters. First (M_1) and second (M_2) modulators: $\lambda_w = 5$ cm, $a_w = 3.71$, respectively 1.6 m and 1.5 m long. The two chicanes $C_{1,2}$ are both 0.45 m long. Radiator: about 20 m long, $\lambda_w = 1.5$ cm, maximum magnetic field: about 1 T.

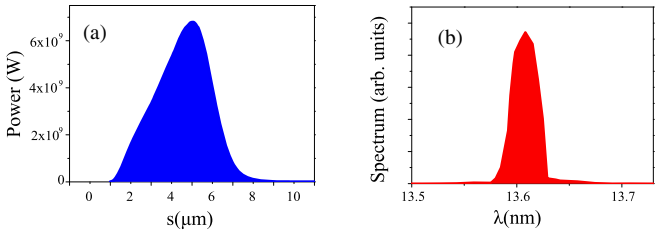

FIG. 2. Signal (a) and spectrum (b) of the intracavity power of the oscillator at saturation.

$$A_{1,2} = \frac{e a_w \lambda_O}{mc^2 \pi \sigma_{1,2}} \sqrt{\frac{P_{1,2}}{c\varepsilon_0 \pi}},$$

$P_{1,2}$ and $\sigma_{1,2}$ being the peak power and the rms transverse dimension of the seeds, e electron charge, m electron mass, c speed of light and ε_0 the vacuum dielectric constant. Assuming $P_{1,2} = 100$, 200 MW respectively (0.86 and 1.72 μJ of total energy), and keeping the longitudinal lengths of the two chicanes constant, $R_{56,1}$ and $R_{56,2}$ have been optimized to maximize the electron bunching on the desired harmonics of the seed. Using an electron energy of 2.66 GeV and a slice relative energy spread of $\Delta E/E = 3 \times 10^{-4}$, proper bunching at the second chicane end is obtained for $n = 25$, corresponding to $\lambda = 5.44$ Å with $R_{56,1} = 132$ μm and $R_{56,2} = 4.72$ μm. The power growth in this case is shown in Fig. 3, its central windows showing the electron phase spaces after the first modulator (a), after the first chicane (b), after the second modulator (c) and at the radiator entrance (d). The initial bunching on $\lambda = 5.44$ Å (in violet) reaches a peak of 4.5% on the bunch, while the rms energy spread increases from 0.03% to 0.045% in the modulators and in the chicanes. These parameters are sufficient to trigger a consistent FEL emission in the radiator, and the radiation is extracted at the minimum bandwidth position, occurring after 12 m of radiator (about 16 m of the total device). The neat single spike structures in power and spectral amplitude at the end of the undulator, are shown in the inner windows in blue and red respectively, compared with the corresponding SASE profiles extracted after 40 m of undulator. Source coherence and stability are evaluated through the modulus of the complex coherence degree:

TABLE II. Characteristics of the seed, generated by the FEL oscillator with undulator length $L_w = 9m$. The repetition rate of the source is 0.5 MHz. \$ = Photons/s/mm^2/mrad^2/bw(‰).

λ_O(nm)	13.6	$E(\mu J)$	70
Photons/shot	4.5×10^{12}	Photons/s	2.27×10^{18}
relative bandwidth	1.7×10^{-3}	rms length(μm)	2
div(μrad)	50	size(μm)	80
peak brilliance(\$)	2.4×10^{31}	average brilliance(\$)	8×10^{22}

$$\Gamma_{ij}(\tau) = \left| \frac{\int dt E_i(t) E_j(t-\tau)}{\sqrt{\int dt |E_i|^2} \sqrt{\int dt |E_j|^2}} \right|,$$

between two different generic pulses i and j generated by different electron beams (Γ_{ij}) or for one single pulse ($\Gamma = \Gamma_{i,i}$), where E_i and E_j are the electric fields of the pulses as function of time. These two quantities are shown vs $\varsigma = c\tau$ for $n = 25$ in the right windows of Fig. 3, together with those of the SASE case at saturation. The FWHM coherence length of the EEHG pulse is $\mathfrak{L}_c = 0.67$ μm, about 4 times the corresponding SASE's. The equal time coherence between different pulses $\Gamma_{ij}(0)$ is close to 1, differently from the SASE's of 10^{-1}. The FWHM mutual coherence length, quantifying the shot-to-shot stability, is 0.1 μm, compared to 0.015 μm of the SASE one. The EEHG coherent source provides an

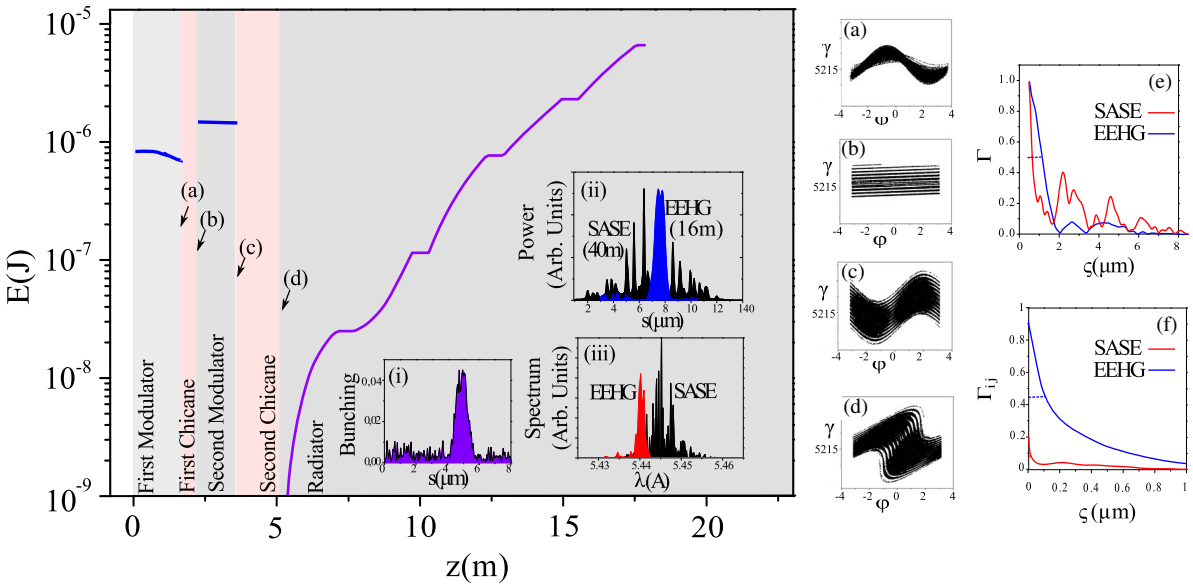

FIG. 3. Radiation energy $E(J)$ vs z(m). In blue, radiation at $\lambda_o = 13.6$ nm in the modulators. In violet, radiation at $\lambda = 13.6/25$ nm $=$ 5.44 Å in the radiator. Point (a) is the 1st modulator end, (b) 1st chicane end, (c) 2nd modulator end and (d) 2nd chicane end. Inner figures: (i) bunching on the 25th harmonics at the end of the 2nd chicane, (ii) power density, (iii) spectral amplitude (SASE at 40 m and EEHG at the radiator exit). Windows (a), (b), (c), (d): electron phase space, electron Lorentz factor γ vs seed phase φ, in the corresponding points. (e) and (f): SASE (red) and EEHG (blue) coherence degree for one pulse Γ and for different pulses Γ_{ij} vs $\varsigma = c\tau$. Dotted segments: FWHM coherence lengths.

ultrashort pulse with 5 μJ of energy per shot at $\lambda = 5.44$ Å, corresponding to 1.4×10^{10} photon/shot at 0.5 MHz or 0.7×10^{16} photons/s, while the SASE source reaches 14.7×10^{16} photons/s at 1 MHz. Even if characterized by a smaller number of photons, bandwidth, coherence and collimation of the EEHG give an average brilliance of 1.7×10^{24} photons/s/mm^2/mrad^2/bw(‰), being only a factor 5 smaller than the corresponding SASE's. Working points covering the range between 5.44 and 2.7 Å, namely $n = 25$, 35, 45, and 50, are presented in Table III and compared to similar SASE cases after 40 m of undulator. Electron beams with progressively larger energies allow to reach shorter wavelengths. Figure 4 presents powers and spectral amplitudes for both SASE (black) and EEHG (red) cases for $n = 35$, 45, 50. The case with $n = 35$ is performed with an electron beam of about 3 GeV and delivers 1.7×10^9 photons/shot at 3.88 Å, extracted after 16 m of radiator with an average brilliance of

TABLE III. SASE (extracted at saturation), EEHG (extracted at minimum bandwidth) and fresh-bunch HGHG cascaded FEL characteristics, \$ = Photons/s/mm^2/mrad^2/bw(‰).

Mode		SASE	EEHG	HGHG	SASE	EEHG	HGHG	SASE	EEHG	SASE	EEHG
Harmonic number			25	5×5		35	7×5		45		50
Wavelength	Å	5.44	5.44	5.44	3.88	3.88	3.88	3.02	3.02	2.72	2.72
γ		5216	5216	5216	6151	6151	6151	6991	6991	7352	7352
Undulator length	m	40	16	32	40	20	32	40	22	40	24
Energy	μJ	58	5.1	7	58	0.9	3.2	46	0.9	42	0.18
Photon/shot	10^9	158	13.9	19	112	1.74	6.2	69	1.36	57	0.245
Bandwidth	0.1%	1	0.37	0.17	0.9	0.4	0.32	0.6	0.3	0.5	0.35
Length	fs	10	1.5	3	10	0.8	4.5	10	1	10	1
Divergence	μrad	3.7	3.9	3.6	2.7	3.2	5.1	2.2	2.5	2.05	2.3
Pulse size	μm	35	27	24	32	25	29	27	25	27	30
Photon/s	10^{15}	158	7	4.7	112	0.87	3.1	69	0.67	57	0.09
Average brilliance	10^{23} \$	94	17	37	151	3.39	5.51	325	5.71	251	0.51
Coherence length	μm	0.17	0.67	1.3	0.11	0.52	1	0.1	0.5	0.1	0.3

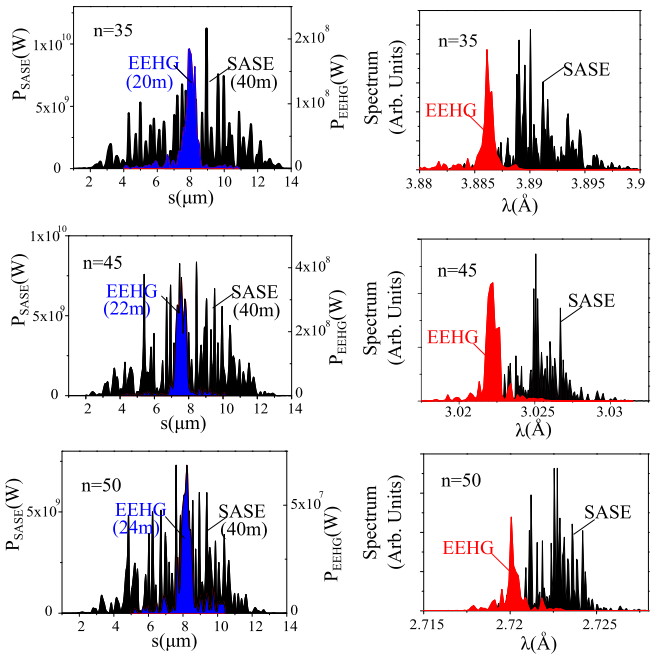

FIG. 4. SASE (black) and EEHG (red) power and spectral radiation profile for $n = 35$ ($R_{56,1} = 184.7$ μm, $R_{56,2} = 4.86$ μm), 45 ($R_{56,1} = 281.6$ μm, $R_{56,2} = 6.58$ μm), and 50 ($R_{56,1} = 293.2$ μm, $R_{56,2} = 6,07$ μm). SASE power vs $s = ct$ is on the left axis, EEHG power on the right. Spectra are in arbitrary units and not in scale.

3.4×10^{23} photons/s/mm^2/mrad^2/bw(‰). With an energy of 3.6 GeV, 1.36×10^9 photons/shot at 3.02 Å ($n = 45$) can be generated with an average brilliance of 5.7×10^{23} photons/s/mm^2/mrad^2/bw(‰). Pushing the electron energy to the maximum value foreseen for MariX, 3.8 GeV, the system produces 2.4×10^8 photons/shot at 2.7 Å ($n = 50$) with a brilliance of 5.7×10^{23}photons/s/mm^2/mrad^2/bw(‰). The coherence length is from 5 ($n = 35$) to 3 ($n = 50$) times the corresponding SASE's, while the stability is larger by a factor from 10 ($n = 35$) to 20 ($n = 50$). Since these estimations widely exceed the target values set by the scientific case, the EEHG source will be capable to satisfy the conditions requested by the envisaged experiments, considering a safety margin compensating all the degradations due to errors, misalignment, jitters and the losses dealing with the transport of the photon beams to the experimental hutch. The comparison between the results of the EEHG technique and those of a fresh-bunch HGHG cascade, performed with a similar electron beam and with the same oscillator as seeding source [14], shows a substantial equivalence in terms of number of emitted photons for $n = 5 \times 5$ and a better performance of the HGHG cascade for $n = 7 \times 5$, when the induced energy spread limits the EEHG radiation. However, the HGHG efficiency decreases very rapidly at higher harmonics ($n > 35$) and radiation levels comparable with the EEHG's cannot be achieved. A total of four different electron bunches per shot are needed for the fresh-bunch technique, while for the EEHG only one bunch for the oscillator and one for the FEL are required, doubling, in proportion, the radiation repetition rate. Regarding coherence, a better performance of the HGHG cascade is observed, due to the more direct transfer of the coherence properties from the seed to the radiation. The advantage of the EEHG is a larger tunability and versatility of the source, that permits to generate intense ($10^{10} - 10^8$ photons/shot), ultrashort (down to 1 fs) pulses at all the harmonics n of the seed up to $n = 50$ and not only at those corresponding to the product of two odd integer numbers ($n = 5 \times 5, 3 \times 9, 7 \times 5 \ldots$).

III. CONCLUSIONS

A new generation accelerator complex is at the core of this coherent and compact facility dedicated and optimized to ultra-fast coherent x-ray spectroscopy and inelastic photon scattering, and to highly penetrating x-ray imaging of mesoscopic and macroscopic samples. The x-ray generation scheme here studied relies on a conventional EEHG device seeded by a far-UV FEL Oscillator and reaching high harmonic orders up to $n = 50$. Its comparison with a SASE FEL performed with a similar electron beam proves the much higher stability and coherence of the produced pulses. The major advantage with respect to a fresh-bunch three-stage FEL cascade seeded by the same oscillator is given by the tunability and simpler setup of the EEHG scheme. Such facility will be intrinsically multiuser and multidisciplinary as of the research performed and science output.

[1] H. Weise and W. Decking, Commissioning and first lasing of the European XFEL, in *Proceeding FEL2017* (2017), MOC03, https://bib-pubdb1.desy.de/record/394127/files/XFEL%20Commissioning.pdf?version=1.

[2] M. L. Grünbein *et al.*, Megahertz data collection from protein microcrystals at an x-ray free-electron laser, Nat. Commun. **9**, 3487 (2018).

[3] E. Allaria *et al.*, Highly coherent and stable pulses from the FERMI seeded free-electron laser in the extreme ultraviolet, Nat. Photonics **6**, 699 (2012).

[4] J. Yan *et al.*, Self-amplification of Coherent Energy Modulation in Seeded Free-Electron Lasers, Phys. Rev. Lett. **126**, 084801 (2021).

[5] L. Giannessi, M. Artioli, M. Bellaveglia, F. Briquez, E. Chiadroni, A. Cianchi *et al.*, High-Order-Harmonic Generation and Superradiance in a Seeded Free-Electron Laser, Phys. Rev. Lett. **108**, 164801 (2012).

[6] G. Geloni, V. Kocharyan, and E. Saldin, A novel self-seeding scheme for hard x-ray FELs, J. Mod. Opt. **58**, 1391 (2011).

[7] J. Amann *et al.*, Demonstration of self-seeding in a hard-x-ray free-electron laser, Nat. Photonics **6**, 693 (2012).

[8] L. H. Yu *et al.*, High-gain harmonic-generation free-electron laser, Science **289**, 932 (2000); A. Doyuran, M. Babzien,

T. Shaftan, L. H. Yu, L. F. DiMauro, I. Ben-Zvi *et al.*, Characterization of a High-Gain Harmonic-Generation Free-Electron Laser at Saturation, Phys. Rev. Lett. **86**, 5902 (2001).

[9] W. Zhang, Commissioning and first lasing of Dalian coherent light source, in *FEL17 Conference* (2017), https://accelconf.web.cern.ch/fel2017/talks/moc04_talk.pdf.

[10] E. J. Takahashi *et al.*, Generation of strong optical field in soft x-ray region by using high-order harmonics, IEEE J. Sel. Topics Quantum Electron. **10**, 6 (2004).

[11] G Lambert *et al.*, An optimized kHz two-colour high harmonic source for seeding free-electron lasers and plasma-based soft x-ray lasers, New J. Phys. **11**, 083033 (2009).

[12] L. Giannessi, M. Bellaveglia, E. Chiadroni, A. Cianchi, M. E. Couprie, M. DelFranco *et al.*, 'Superradiant Cascade in a Seeded Free-Electron Laser', Phys. Rev. Lett. **110**, 044801 (2013).

[13] M. Labat, M. Bellaveglia, M. Bougeard, B. Carre, F. Ciocci, E. Chiadroni *et al.*, High-Gain Harmonic-Generation Free-Electron Laser Seeded by Harmonics Generated in Gas, Phys. Rev. Lett. **107**, 224801 (2011).

[14] V. Petrillo *et al.*, Coherent, high repetition rate tender x-ray free-electron laser seeded by an extreme ultraviolet free-electron laser oscillator, New J. Phys. **22**, 073058 (2020).

[15] S. Ackermann, B. Faatz, V. Grattoni, M. M. Kazemi, T. Lang, C. Leclmer, G. Paraskaki, and J. Zemella, Novel method for the generation of stable radiation from free-electron lasers at high repetition rates, Phys. Rev. Accel. Beams **23**, 071302 (2020).

[16] G. Dattoli, E. Di Palma, and A. Petralia, Free-electron laser oscillator efficiency, Opt. Commun. **425**, 29 (2018).

[17] F. Ciocci, G. Dattoli, A. De Angelis, B. Faatz, F. Garosi, L. Giannessi, P. L. Ottaviani, and A. Torre, Design considerations on a high-power VUV FEL, IEEE J. Quantum Electron. **31**, 1242 (1995).

[18] P. J. M. Van der Slot, H. P. Freund, W. H. Miner, Jr., S. V. Benson, M. Schinn, and K.-J. Boller, Time-dependent Three Dimensional Simulation of Free-Electron Laser Oscillators, Phys. Rev. Lett. **102**, 244802 (2009).

[19] K.-J. Kim and Y. Shvyd'ko, Tunable optical cavity for an x-ray free-electron laser oscillator, Phys. Rev. ST Accel. Beams **12**, 030703 (2009).

[20] K.-J. Kim, Y. Shvyd'ko, and S. Reiche, A Proposal for an X-ray Oscillator with an Energy Recovery Linac, Phys. Rev. Lett. **100**, 244802 (2008).

[21] V. Petrillo *et al.*, High repetition rate and coherent free-electron laser in the x-rays range tailored for linear spectroscopy, Instruments **3**, 47 (2019).

[22] Z. Huang and R. D. Ruth, Fully Coherent X-Ray Pulses from a Regenerative-Amplifier Free-Electron Laser, Phys. Rev. Lett. **96**, 144801 (2006).

[23] B. W. J. McNeill, N. R. Thomson, D. J. Dunning, J. G. Karssenber, P. J. M. Van der Slot, and K.-J. Boller, A design for the generation of temporaly-coherent radiation pulses in the VUV and beyond by a seld-seeded high gain free electron laser amplifier, New J. Phys. **9**, 239 (2007).

[24] K. Li and H. Deng, Systematic design and three-dimensional simulation of x-ray FEL oscillator for Shanghai Coherent Light Facility, Nucl. Instrum. Methods Phys. Res., Sect. A **895**, 40 (2018).

[25] G. Marcus, Y. Ding, A. Halavanau, Z. Huang, J. Krzywinski, J. MacArthur, R. Margraf, T. O. Raubenheimer, D. Zhu, and V. Fiadon, Regenerative amplification for a hard-x ray free-electron laser, in *Procedings FEL 2019*, TUP032, https://accelconf.web.cern.ch/fel2019/papers/tup032.pdf.

[26] G. Marcus *et al.*, Cavity-based free-electron laser research and development: A Joint Argonne National Laboratory and SLAC National Laboratory collaboration, in *Proceedings FEL 2019*, TUD04, https://accelconf.web.cern.ch/fel2019/papers/tud04.pdf.

[27] K. Li, J. Yan, C. Feng, M. Zhang, and H. Deng, High brightness fully coherent x-ray amplifier seeded by a free-electron laser oscillator, Phys. Rev. Accel. Beams **21**, 040702 (2018).

[28] G. Stupakov, Using the Beam-Echo Effect for Generation of Short-Wavelength Radiation, Phys. Rev. Lett. **102**, 074801 (2009).

[29] D. Xiang and G. Stupakov, Echo-enabled harmonic generation free electron laser, Phys. Rev. ST Accel. Beams **12**, 030702 (2009).

[30] E. Hemsing, M. Dunning, B. Garcia, C. Hast, T. Raubenheimer, G. Stupakov, and D. Xiang, Echo- enabled harmonics up to the 75th order from precisely tailored electron beams, Nat. Photonics **10**, 512 (2016).

[31] C. Feng, H. Deng *et al.*, Coherent extreme ultraviolet free-electron laser with echo-enabled harmonic generation, Phys. Rev. Accel. Beams **22**, 050703 (2019).

[32] P. R. Ribič *et al.*, Coherent soft x-ray pulses from an echo-enabled harmonic generation free-electron laser nature research, Nat. Photonics **13**, 1 (2019).

[33] J. Wurtele, P. Gandhi, and X.-W. Gu, Tunable soft x-ray oscillators, in *Proceedings of the 32nd Free Electron Laser Conference, Malmö, Sweden* (Max-lab, Sweden, 2010).

[34] L.Serafini *et al.*, MariX, an advanced MHz-class repetition rate X-ray source for linear regime time-resolved spectroscopy and photon scattering, Nucl. Instrum. Methods Phys. Res., Sect. A **930**, 167 (2019).

[35] A.Bacci, M. R. Conti, A. Bosotti, S. Cialdi, S. Di Mitri, I. Drebot, L. Faillace *et al.*, Two-pass two-way acceleration in a super-conducting CW linac to drive low jitters x-ray FELs, Phys. Rev. Accel. Beams **22**, 111304 (2019).

[36] S. Di Mitri and M. Cornacchia, Transverse emittance-preserving arc compressor for high brightness electron beam-based light sources and colliders, Europhys. Lett. **109**, 62002 (2015); S. Di Mitri, Feasibility study of a periodic arc compressor in the presence of coherent synchrotron radiation, Nucl. Instrum. Methods Phys. Res., Sect. A **806**, 184 (2016).

[37] M. Placidi, S. Di Mitri, C. Pellegrini, and G. Penn, Compact FEL-driven inverse Compton scattering

gamma-ray source, Nucl. Instrum. Methods Phys. Res., Sect. A **855**, 55 (2017).

[38] A. Vostrikov, A. Sukhanov, V. Yakovlev, and N. Solyak, Cumulative HOM excitation and transition effects in LCLS-II, Phys. Procedia **79**, 46 (2015).

[39] S. Reiche, GENESIS 1.3: a fully 3D time-dependent FEL simulation code, Nucl. Instrum. Methods Phys. Res., Sect. A **429**, 243 (1999).

[40] F. Capotondi *et al.*, Multipurpose end-station for coherent diffraction imaging and scattering at FERMI@Elettra free-electron laser facility, J. Synchrotron Radiat. **22**, 544 (2015).

[41] J. Bodewadt, J. RoBdach, and E. Hass, Commissioning results of the photon-electron diagnostic unit at SFLASH, in *Proc. of DIPAC2011* (2011), MOPD54.